The 15th International Symposium on Magnetic Bearings, August 3-6, 2016, Mojiko Hotel, Kitakyushu, Japan

ISMB15

Design Consideration for Performance Improvement in One-Axis Actively Positioned Single-Drive Bearingless Motor

Hiroya SUGIMOTO*, Itsuki SHIMURA* and Akira CHIBA*

*Dept. of Electrical and Electronic Engineering, Tokyo Institute of Technology

2-12-1 Ookayama, Meguro, Tokyo 152-8550, Japan

E-mail: sugimoto@belm.ee.titech.ac.jp

Abstract

This paper presents rotor structures to enhance the active axial force in a single-drive bearingless motor. The single-drive bearingless motor can generate both torque and active axial force by q- and d-axis currents, respectively, with only one three-phase inverter. The axial *z*-axis position is actively regulated, but the other axes, radial and tilting movements, are passively stabilized. In this paper, the rotor structure is improved to enhance the active axial force. The active axial force and the other important performance parameters are calculated in three-dimensional finite-element-method analysis. In addition, the performance is comprehensively evaluated.

Keywords : bearingless motor, magnetic bearing, one degree-of-freedom, single-drive, permanent magnet machine

1. Introduction

Bearingless motors have two functions of a rotating machine and a magnetic bearing. Therefore, the advantages are no wear, no lubricant, non-pollution, maintenance-free and long life-time because the rotor shaft is magnetically suspended without mechanical bearings. Thus, the bearingless motors have been studied for industry applications such as centrifugal pumps, contamination-free ventricular assist devices, high purity pharmaceutical mixing devices, compressors, rotating stages, flywheels and cooling fans.

One of the important issues in bearingless motors is high cost for magnetic suspension. In case of conventional five-axis actively positioned bearingless motors, radial, tilting and axial directions are actively positioned. Therefore, five displacement sensors, three three-phase inverters and one single-phase inverter are required for generating motor torque and suspension forces. As a result, the cost is quite high. For reducing the cost reduction of the number of actively positioning axes is effective. In one-axis actively positioned magnetic bearing motors and bearingless motors [1]-[11], only axial direction *z* is actively positioned, thus, only one displacement sensor and two or less number of inverters are necessary. The other axes are passively stabilized by passive magnetic bearing functions. In particular, when single-drive bearingless motor concept is applied, only one displacement sensor and one three-phase inverter are necessary. Therefore, the cost is extremely reduced. Thus, the authors have studied the single-drive bearingless motors in [10] and [11].

Fig. 1 shows a proposed single-drive bearingless motor for cooling fan applications. The improvement of torque density is one of the most important issues. Normally, the torque density is decreased when the magnetic bearing function is integrated because the machine volume is increased. However, the torque density should be improved for the industry applications. In [4], [8]-[9], the torque densities have been improved. The authors have

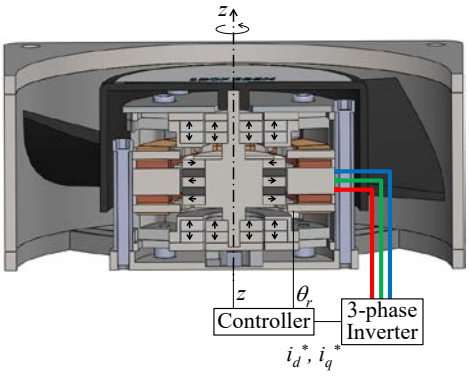

Fig. 1. Proposed single-drive bearingless motor for cooling fan applications.

also improved the torque density with high radial stiffness in [11].

In this paper, the rotor structure is improved to enhance the active axial force and to reduce rare-earth material in the permanent magnets. In three-dimensional finite-element-method (3D-FEM) analysis, the active axial force, unstable radial attraction force and unstable axial attraction force are calculated. In addition, the performances are comprehensively evaluated.

2. Previously proposed single-drive bearingless motor

Fig. 2 shows the previously proposed structure of the single-drive bearingless motor in [11]. The structure has a single-drive bearingless motor between two repulsive passive magnetic bearings. In the center, the stator and the rotor of a bearingless motor are constructed with three layers. In the center layer, the active axial force and the rotational torque are generated. In the upper and lower layers, only active axial force is generated because the torque is canceled between the upper and lower layers. The rotor has permanent magnets for eight rotor poles. The magnetized directions in the center and lower layers are the identical. In contrast, the magnetized direction in the upper rotor is opposite to the other layers. The stator is constructed with three laminated cores and two ring yokes. The materials of the laminated core and the ring yoke are silicon steel 35H360 and carbon steel S45C, respectively. Only one set of three-phase eight-pole winding is wound around the center stator core.

Fig. 3 shows a power electronics circuit in the proposed single-drive bearingless motor. A three-phase inverter is connected to the three-phase winding. Thus, the inverter topology is just identical with typical three-phase brushless DC motors.

Fig. 4 shows *xy* cross-sectional view at the center layer core. The rotor has eight permanent magnets magnetized in parallel radial directions so that the number of rotor poles is eight. The permanent magnets are installed in a holder which is shown as a blue part in Fig. 4. The material of the holder is not iron core but plastic. The stator has twelve slots and teeth with one set of three-phase eight-pole concentrated winding. Thus, the cross-sectional view is a typical surface permanent magnet (SPM) motor structure. The rotor outer diameter and magnetic gap are 27 mm and 0.8 mm, respectively.

Fig. 5 shows principle of the active axial force generation in the proposed structure. Only *xz* cross-sectional view of the center part in Fig. 2 is illustrated. The active axial force and the torque are generated by the *d*-axis and *q*-axis

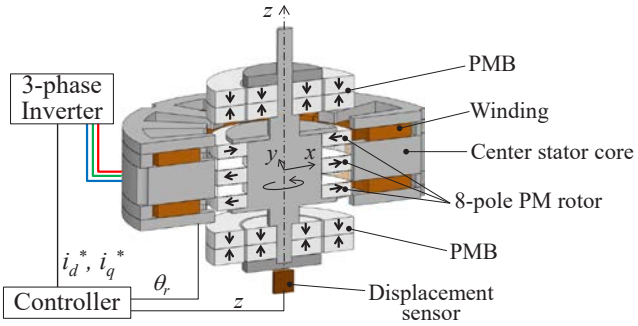

Fig. 2. Previously proposed structure.

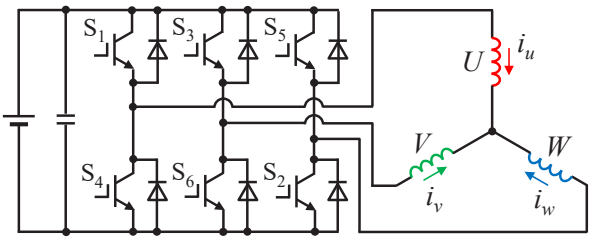

Fig. 3. Power electronics circuit in single-drive bearingless motor.

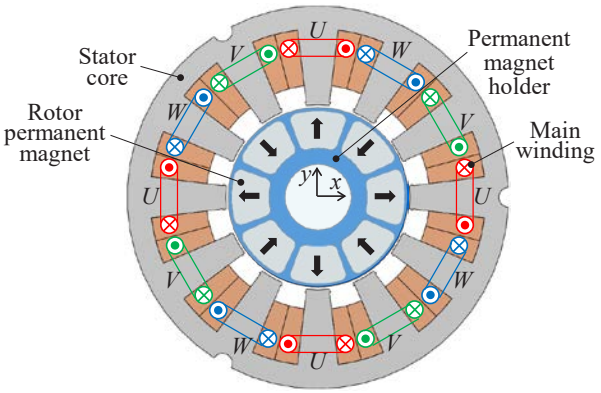

Fig. 4. Winging arrangement in *xy* cross-sectional view.

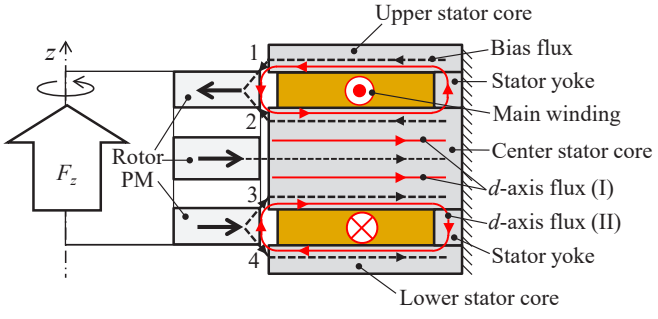

Fig. 5. Principle of active axial force generation.

currents, respectively. The rotor rotational angular position in Fig. 5 is corresponding to the *d*-axis. Solid black arrows indicate the magnetized direction of the rotor permanent magnets. Black broken curves indicated as bias fluxes show the permanent magnet flux paths. The permanent magnet fluxes pass through the air-gap, and radially circulate in the stator core. The upper and lower permanent magnet fluxes have *z*-axis direction components in the air-gap because the rotor permanent magnets are installed at unaligned positions with respect to the stator teeth. There are two d-axis flux paths (I) and (II) indicated as red arrows. The d-axis fluxes (I) are radially circulated, thus, the active axial force is not generated, but typical flux intensifying. The d-axis fluxes (II) are important to generate the active axial force. Through the center stator core and the stator yoke, the *d*-axis fluxes (II) are circulated and go to the upper and lower stator cores. In the air-gap, the *d*-axis fluxes (II) also have *z*-axis direction components. The *d*-axis fluxes (II) are superimposed on the permanent magnet bias fluxes. When the *d*-axis current is positive, the flux densities are increased in the air-gap 1 and 3 because the bias flux and the d-axis fluxes (II) are intensified. At the same time, the flux densities are weakened in the air-gap 2 and 4. As a result, the positive axial force is generated. In case of negative *d*-axis current, negative axial force is generated.

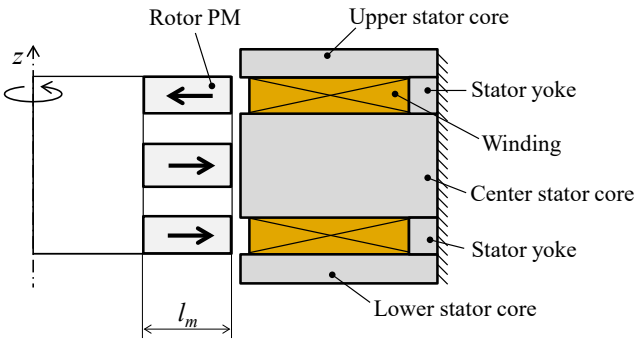

(a) Structure A

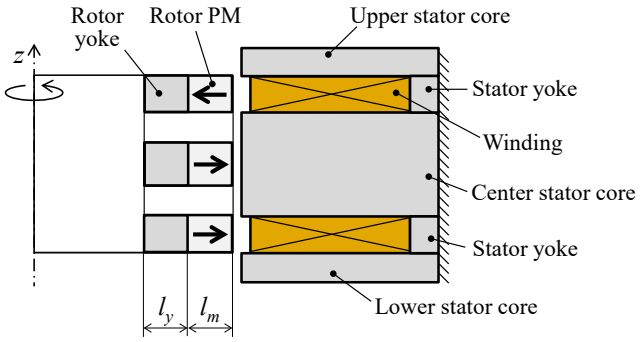

(b) Structure B

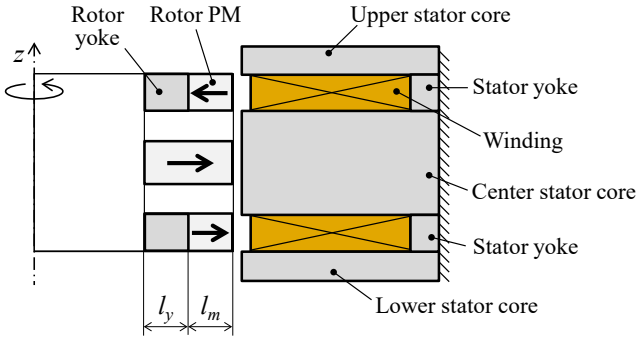

(b) Structure C

Fig. 6. *xz* cross-sectional view of (a) previous structure, (b) improved structure with rotor yoke inside rotor permanent magnet in each layer and (c) with rotor yoke in upper and lower layers.

3. Improved rotor structure with back yoke

Fig. 6 (a), (b) and (c) show *xz* cross-sectional views of the previous structure and two improved structures. In Fig. 6 (a), the rotor is constructed with permanent magnets and the rotor shaft. The thickness l_m of the permanent magnet is 6 mm. The shaft is installed inside of the rotor permanent magnet. The shaft material is non-magnetic stainless steel SUS304. In Fig. 6 (b), back yokes are installed on the rotor permanent magnets in each three layers. The back yoke is constructed with laminated silicon steel. In this paper, the thickness l_m and l_y of the permanent magnet and the back yoke are identical length of 3 mm. In Fig. 6 (c), the back yoke is installed on the upper and lower rotor permanent magnets. Both the thickness l_m and l_y are 3 mm. On the other hand, the thickness of the center permanent magnet is 6 mm. When the back yoke is installed on the permanent magnet, it is expected that the active axial force is increased because flux linkages in the upper and lower stator cores are increased by reduction of the magnetic resistance.

4. 3D-FEM analysis

Fig. 7 shows the active axial force with respect to d-axis current. In this calculation, the number of winding per tooth is 74. The material in the rotor permanent magnet is N40SH. In the calculation result, the current-force factor in the previous structure A is 2.2 N/A. In case of the structures B and C, the current-force factors are improved by 3.1 and 3.2 N/A, respectively. In this design, rated RMS current is 1 A. When the d-axis current is increased up to five times of

the rated current, maximum active axial forces in the three structures are 14.5 N, 19.6 N and 20.3 N, respectively. Therefore, the rotor back yoke is effective to enhance the active axial force.

Fig. 8 shows the unstable radial magnetic attraction force with respect to the rotor radial displacement. In case of the structure B, unfortunately, negative radial stiffness is increased by 1.9 times compared with the structure A. The back yoke on the center rotor permanent magnet causes high negative radial stiffness. In case of the structure C, the negative radial stiffness is slightly increased compared with the structure A. However, the negative stiffness is rather low compared with the structure B. When the negative radial stiffness is high, high positive radial stiffness is necessary to stabilize the radial direction. Therefore, the passive magnetic bearing must be enlarged. In the worst case, the rotor can not be stabilized because the negative axial force is increased. Hence, low negative radial stiffness is better for the single-drive bearingless motors.

Fig. 9 shows the unstable axial magnetic attraction force with respect to the rotor axial displacement. Similar to the negative radial stiffness, the negative axial stiffness is also increased compared with the structure A due to the rotor back yoke. The negative axial stiffness in the structure B and C are mostly same value.

From the negative radial stiffness and negative axial stiffness, target active axial force is estimated to achieve start-up from touch-down [11]. Let us define the negative radial stiffness and negative axial stiffness as k_{rc} and k_{zc}, respectively. In addition, let us define positive radial stiffness in the repulsive passive magnetic bearing and total radial stiffness as k_{rp} and k_r, respectively. Thus, total negative axial stiffness k_z is given as follows:

$$k_{rp} = k_r - k_{rc}\,, \tag{1}$$

$$k_z = -2ak_{rp} + k_{zc}\,. \tag{2}$$

where let us suppose a safety coefficient a as 1.4. Therefore, when maximum axial displacement at start-up is z_{max}, the target active axial force F_{zt} is given as follows:

$$F_{zt} = -k_z z_{max}\,. \tag{3}$$

Therefore, when the negative radial stiffness is high, high target force is required in constant total radial stiffness. In this paper, the maximum axial displacement is 0.1 mm.

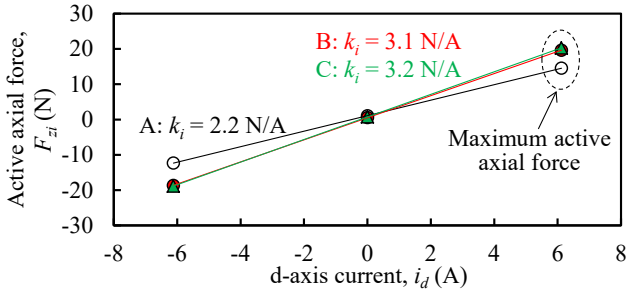

Fig. 7. Active axial force with respect to d-axis current.

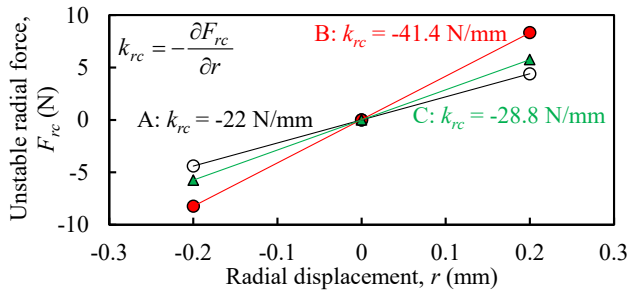

Fig. 8. Unstable radial magnetic attraction force.

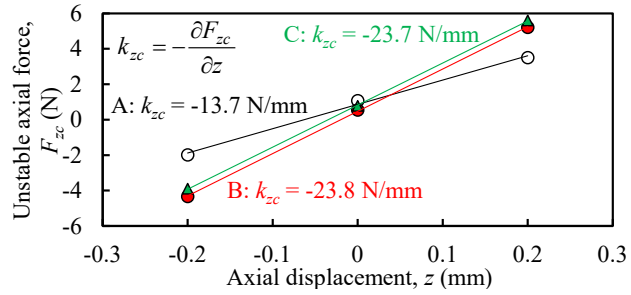

Fig. 9. Unstable axial magnetic attraction force.

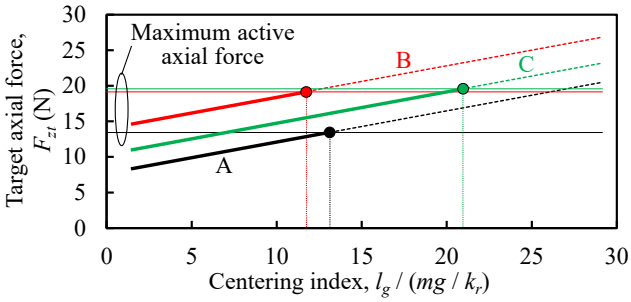

Fig. 10. Available region of centering index.

Fig. 10 shows the target active axial force with respect to a centering index. Let us define the centering index as a ratio of magnetic gap length l_g and the rotor radial eccentricity mg / k_r caused by the rotor weight mg. High centering index is better because of low rotor radial eccentricity. When the total radial stiffness k_r is increased, the centering index is also increased. As a result, the positive radial stiffness k_{rp} is increased in (1), therefore, the target active axial force is increased. Thus, the target force is proportional to the centering index in Fig. 10. The target force in the structure B is the highest because the negative radial stiffness is high. Therefore, available centering index is rather low compared with the structure A and C although the structure B can generate high maximum active axial force. Consequently, the structure C is the best choice because high active axial force and high centering index can be achieved.

5. Conclusion

This paper presents a rotor structure improvement in a single-drive bearingless motor. Installation of the back yoke in the upper and lower rotors is effective to enhance the active axial force. In addition, high centering index can be achieved in the proposed rotor structure because low negative radial stiffness.

References

[1] I. D. Silva, J. R. Cardoso, and O. Horikawa, "Design Considerations for Achieving High Radial Stiffness in an Attraction-Type Magnetic Bearing With Control in a Single Direction," *IEEE Trans. Magn.*, vol. 47, no. 10, pp. 4112–4115, Oct. 2011.

[2] J. Kuroki, T. Shinshi, L. Li, and A. Shimokohbe, "Miniaturization of a one-axis-controlled magnetic bearing," *Precis. Eng.*, vol. 29, no. 2, pp. 208–218, Apr. 2005.

[3] J. Asama, Y. Hamasaki, T. Oiwa, and A. Chiba, "Proposal and Analysis of a Single-Drive Bearingless Motor", *IEEE Trans. Industrial Electronics*, vol. 60, no. 1, pp. 129-138, Jan. 2013.

[4] J. Asama, D. Watanabe, T. Oiwa, and A. Chiba, "Development of a One-Axis Actively Regulated Bearingless Motor with a Repulsive Type Passive Magnetic Bearing", *in Proc. International Power Electronics Conference (IPEC-Hiroshima2014-ECCE-ASIA)*, pp.988-993, 2014.

[5] S. Yang and M. Huang, "Design and Implementation of a Magnetically Levitated Single-Axis Controlled Axial Blood Pump", *IEEE Trans. Industrial Electronics*, vol. 56, no. 6, pp. 2213-2219, Jun. 2009.

[6] Q. D. Nguen and S. Ueno, "Modeling and control of salient-pole permanent magnet axial-gap self-bearing motor," *IEEE/ASME Trans. Mechatronics*, vol. 16, no. 3, pp. 518–526, Jun. 2011.

[7] T. Ohji, Y. Katsuda, K. Amei, and M. Sakui, "Structure of One-Axis Controlled Repulsive Type Magnetic Bearing System With Surface Permanent Magnets Installed and Its Levitation and Rotation Tests", *IEEE Trans. Magn.*, vol. 47, no. 12, pp. 4734-4739, Dec. 2011.

[8] W. Bauer and W. Amrhein, "Electrical Design Considerations for a Bearingless Axial-Force/Torque Motor", *IEEE Trans. Ind. Appl.*, vol. 50, no. 4, pp. 2512–2522, July/August 2014.

[9] W. Bauer, P. Freudenthaler, and W. Amrhein, "Experimental Characterization of a Bearingless Rotating Field Axial-Force/Torque Motor", *in Proc. 14th International Symposium on Magnetic Bearings (ISMB14)*, Linz, Austria, pp.132-137, 2014.

[10] H. Sugimoto, S. Tanaka, A. Chiba, and J. Asama, "Principle of a Novel Single-Drive Bearingless Motor with Cylindrical Radial Gap", *IEEE Trans. Ind. Appl.*, vol. 51, no. 5, pp.3696-3709 , Sep./Oct., 2015.

[11] H. Sugimoto, I. Shimura, and A. Chiba, "Design of SPM and IPM Rotors in Novel One-Axis Actively Positioned Single-Drive Bearingless Motor", *in Proc. Energy Convers. Congr. and Expo. (ECCE2014)*, pp. 5858-5863, 2014.